Photon Production in Au + Au collisions at $\sqrt{s_{NN}}$ = 130 *GeV*

Ian Johnson, Masashi Kaneta and James Symons, *Lawrence Berkeley National Laboratory*
for the STAR Spectra/High pt Physics Working Groups and the STAR Collaboration

ABSTRACT

Results are presented for inclusive photon yields from Au+Au collisions at RHIC. Photons in the energy range from 100 MeV – 4 GeV have been detected by reconstructing conversion pairs in the STAR TPC. Energy resolution, purity, and detection efficiency are discussed. Prospects for extracting cross sections of relevant photon production processes, such as the $\pi^0 \rightarrow \gamma\gamma$, are presented.

A Typical Event

rz view of the e+ and e- tracks for photon conversion candidates

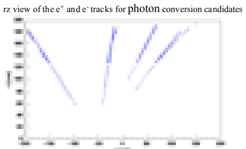

xy view of the e+ and e- tracks for photon conversion candidates

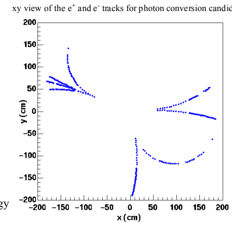

The dominant interaction process for photons of energy greater than 10 MeV is conversion of the γ-ray to an electron-positron pair in the field of a nucleus. The average angle between the direction of emission of the created electron or positron is $\theta \sim mc^2/E$. Thus, the characteristic signature of a γ-ray conversion will be a pair of tracks with very small opening angle pointing back towards the primary reaction point. This is illustrated in the figure above, which shows the hits associated with four conversion candidates from a single central event. The hits associated with the ~600 primary tracks are not shown.

Candidate Selection

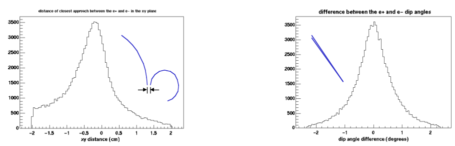

Photon candidates are found by searching for pairs of tracks which have the characteristics expected for the conversion process. The algorithm first calculates the distance of closest approach between tracks of opposite helicity (shown in the left figure, xy plane). The dip angles of the two tracks in the candidate pair are then compared in order to select pairs with small opening angle. The right figure displays the dip angle difference. The measured widths of these distributions are limited by the tracking resolution of the time projection chamber. The actual opening angle of the photons in our sample is expected to be a tenth of a degree or less. For the figures shown below, selection cuts were placed at ±1.4 cm for the separation and at ±1° for the dip angle difference.

Primary Photon Selection

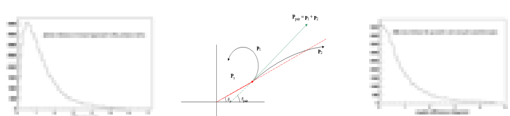

Photons that originate from sources other than the primary interaction are rejected by cuts on the pair momentum. This is done in two different ways. First, a distance of closest approach (dca) to the primary vertex is calculated by projecting the photon's path back to the primary vertex. The dca distribution is shown in figure (a). Secondly, we calculate the difference in angle between the reconstructed momentum vector of the photon and the geometric vector from the primary vertex to the conversion point as illustrated in figure (b). The measured angular differences are shown in figure (c). These two figures clearly show that there is very little background from sources other than the primary interaction point, which would produce a flat background under the peak from 'primary' pairs.

Purity and Confidence

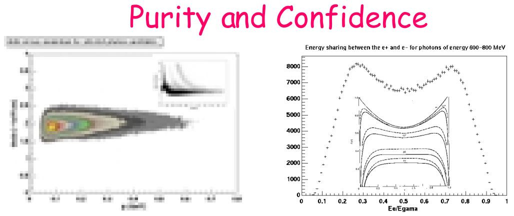

After the photon candidates have been refined with geometric and energetic cuts. Additional confidence in the purity of the sample come from particle identification on the conversion daughters. The left plot illustrate the purity of the electron and positron dedx. In the main frame, only selected candidates daughters dedx is plotted versus momentum. In the small inlay is the dedx spectrum for the initial mixture of all particles in the events. Comparing these two plots clearly shows a high purity of electrons and positron in the selected sample. The right plot displaces the energy sharing between the electron and positron. In the expected flat acceptance region ($.25 < E_e/ E_\gamma < .75$) the uncorrected distribution reproduces the theory (inlay) nicely.

A Detector X-ray

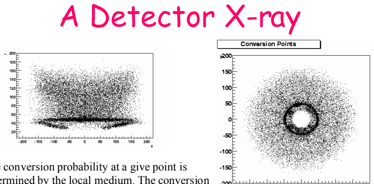

The conversion probability at a give point is determined by the local medium. The conversion probability increases with density and Z of a material. In the two plots photon conversion points are used to map out the material of the detector.

Efficiency

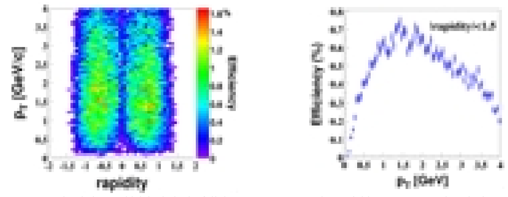

GEANT Simulations, which include the full detector geometry and material layout, were used to obtain these efficiency corrections. The input photon distribution was flat in transverse momentum(p_T) and rapidity. The p_T range stretches from $0 < p_T < 4$ GeV/c and the rapidity range is from $-2 < y < 2$. The left plot illustrates the efficiency in a two dimensional contour of p_T versus rapidity. The right plot displays the efficiency as a function of p_T.

Simulated Resolution

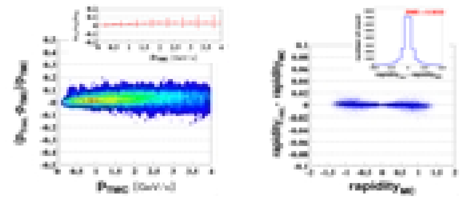

Resolution studies were obtained by using GEANT simulations. In the figures p_{TMC} is *input transverse momentum* and p_{Trec} is *reconstructed transverse momentum* . The p_T resolution is 3% up to 1 GeV/c and less than 10% at 4GeV/c. The rapidity resolution is 0.0033 for |y|<1.5.

Uncorrected Spectra

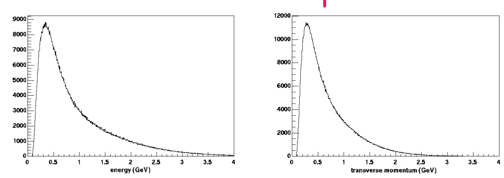

Various physical spectra can be made and analyzed with a pure, confident sample of primary photons. These plots are distributions directly taken from the data. They have not been corrected with the above efficiency and acceptance corrections. The left figure shows the uncorrected photon energy distribution. The right figure shows the uncorrected transverse energy distribution.

Two Photon Invariant Mass Spectrum

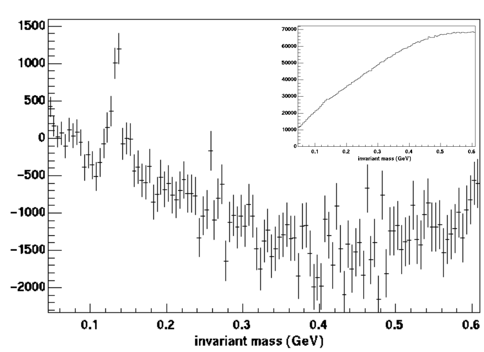

There are hints of structure in the invariant mass spectrum (inlay) at the mass of the π^0. However after subtraction of a mixed event background, a statistically significant peak is clearly visible (main frame). Since the majority of primary photons are expected to come from π^0 decay, the possibility of constructing the invariant mass of $\gamma\gamma$ pairs to measure the π^0 cross section is extremely important. At first sight, this would seem very unpromising with our technique: the efficiency for detecting a single photon is of the order of 1%, thus one will detect both γs from a π^0 decay with an efficiency of 1 in 10000. In addition, because of the high π^0 density in RHIC events, there is an enormous combinatoric background. However, it is important to remember that the peak to background ratio is determined by the π^0 phase space density and the energy resolution of the detector, not by the efficiency. The only drawback of low efficiency is that one has to accumulate many events, to obtain statistical significance. STAR had an energy resolution of ~3% for photons of a few hundred MeV in the 2000 run, because the detector was operated at half field. In 2001, the resolution is expected to improve by a factor of 2. The figures above are our first calculation of the $\gamma\gamma$ invariant mass for the year 2000 data set.

Future Goals

The energetic range and, energy and directional resolution of this photon detection method compensate for the low detection efficiency. This compensation gives light to a broad range of future goals. Among these goals are the measurement of the inclusive photon cross section, the measurement of the π^0 cross section, the detection of Σ^0 via $\Lambda^0\,\gamma$ decay channel, a measurement of the upper limit of direct photon production, and studies relevant to Disoriented Chiral Condensates.